

# AN EFFICIENT INVERSE AERODYNAMIC DESIGN METHOD FOR MULTI COMPONENT DEVICES

Kisa Matsushma\*, Masahi Shiokawa\*, Kazuhiro Nakahashi\*

\*Dept. of Aeronautics and Space Engineering and Sciences, Tohoku University,

**Keywords:** *Inverse problems, Multi-wing, CFD, Aerodynamic design, Interaction*

## Abstract

An aerodynamic design system using an advanced inverse problem is proposed. The inverse problem can handle multi components of wing-like-shape that mutually interact with each other. The system determines each component's shape simultaneously which will realize desired pressure distribution. In the design system, the inverse problem is coupled with Navier-Stokes flow analysis code. Thus the design result is valid for Navier-Stokes flows, while the inverse problem uses potential flow approximation. The typical multi component example of a high-lift device has been designed as demonstration. The result has indicated that the present method works well, and can precisely control geometry with constraints. It has been also shown that the method is flexible as well as cost and time efficient.

## Nomenclature

$x, y, z$  Cartesian coordinate system of a flowfield with wings.  $x$ ; stream-wise,  $y$ ; span-wise,  $z$ ; thickness-wise or altitude direction.

$\xi, \eta, \zeta$  coordinate system for Green's integration corresponding to  $x, y$  and  $z$ , respectively.

$k_{max}$  number of components or wings in a flowfield to be designed.

$\gamma$  ratio of specific heats (=1.4)

$M_\infty$  free stream Mach number

$K$  transonic similarity parameter  
 $=(\gamma+1) M_\infty^2$

$\beta$  the Prandtl-Glauert constant;  
 for incompressible flow =1.0

for compressible flow  $= (1.0 - M_\infty^2)^{1/2}$

$\phi(x,y,z)$  small perturbation velocity potential

$\Delta\phi(x,y,z)$  variation of  $\phi(x,y,z)$  due to shape modification.

$f_k(x,y)$  geometry of  $k$ th component (wing); its surface coordinate is  $(x, y, f_k(x,y))$ .

$f_{k+}(x,y)$  upper surface geometry of  $k$ th component.

$f_{k-}(x,y)$  lower surface geometry of  $k$ th component.

$\Delta f_{k\pm}(x,y)$  modification value of  $f_{k\pm}(x,y)$

$C_p(x,y)$  surface pressure coefficient,  $C_p$ , distribution.

$\Delta C_p(x,y)$  difference between target  $C_p$  and current  $C_p$

$c_k$   $z$  location of the mean plane of  $k$ th component

$c_{k+0}$   $z$  location of the upper surface of  $k$ th component.

$c_{k-0}$   $z$  location of the lower surface of  $k$ th component

(Subscript)

$k$  quantity concerning  $k$ th component.

$+$  quantity on an upper surface.

$-$  quantity on a lower surface..

## 1 Introduction

Multi-wing systems are important to enhance aerodynamic performance of aircraft. Multi-element airfoils/wings, a slat, a main part and several flaps, take a crucial role for generating high-lift<sup>(1)</sup>. Tandem wings are interesting for developing special-purpose aircraft. The tri-surface system of a canard, a main wing and a tail wing is under research to improve

performance and controllability for the maneuver of aircraft<sup>(2,3)</sup>. The bi-plane theory originated from Plandtl long time ago is still attracting<sup>(4)</sup>, but has not been applied to conventional aircraft development.

In these days, stimulating by the progress of computational fluid dynamics (CFD), the design and development strategy of new aircraft has been gradually changed. The knowledge obtained from CFD solutions can cut down windtunnel workload as well as preliminary design costs. Among CFD techniques, a design method using an inverse problem solver is very practical for the design of airfoils and wings because it is efficient and precisely controllable. In this article, a design system using an advanced inverse problem is proposed. The inverse problem can handle multi components of wing-like-shape that mutually interact with each other. So, the system determines each component's shape simultaneously which will realize desired pressure distributions. The typical multi component example is high-lift devices. Design of high-lift devices is one of most significant subjects for aircraft development in terms of the aerodynamic performance improvement<sup>(1)</sup>. However, usual optimizations need a lot of times to calculate flows around those geometrically complicated subjects. That is too long for realistic design purpose. An economical, efficient and effective design system is desired.

## 2 Aerodynamic Design Method

### 2.1 Design Object - Multi component System

The function of the present design method is to determine the section shapes at any span-station of plural wings/components which interact with each other (Fig. 1). At each span-station, the airfoil contour and twisting angle are properly changed to satisfy the specified aerodynamic performance which is expressed via a pressure distribution along the chord-wise,  $x$  direction.

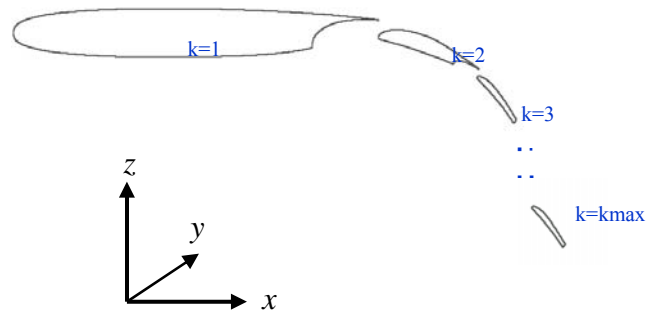


Fig. 1 Sections of multi component system.

### 2.2 Residual-Correction Concept

The method attains to the goal asymptotically by iterating a "residual-correction" loop. The residual is defined as the difference between the target and current pressure distributions. The correction is made on the wing geometry to make up for the residual. Figure 2 illustrates the design flow. Design starts with an initial geometry and a target pressure distribution which should lead to the desired aerodynamic performance. The successive iteration of Navier-Stokes flow analysis and inverse design to determine the geometry correction provides the design result of each component. The system can deal with design constraints such as component's thickness and Gaps between any two components. It can handle two and three dimensional design problems.

This procedure has two primary parts; one is flow analysis, where grid generation and flow simulation are conducted. For the analysis part, any kind of simulation code can be employed or even a windtunnel test can replace the computational analysis, as long as it provides a reasonably accurate pressure distribution on the wing surface. The other primary part is an inverse design part where the mathematical inverse problem, i.e. the integral equation system, is solved to update the wing geometry. The design part provides the correction value for asymptotic approach to a solution. The present research addresses the design part. To formulate the inverse problem for the design part in the residual-correction loop, we consider

two flowfields; a current and the target.

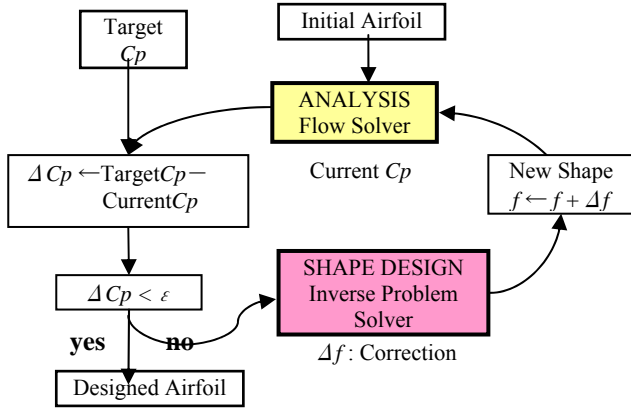


Fig. 2 Design system outline.

A current wing geometry is  $f_k(x,y)$  and The pressure distribution corresponding to the current wing geometry is  $Cp(x,y)$ . In the target flowfield, wing geometry is modified such as, new  $f_k(x,y) = f_k(x,y) + \Delta f_k(x,y)$ , so that new  $f_k(x,y)$  can realize the specified target pressure distribution. The inverse problem solve the equation to determine geometric correction  $\Delta f_k(x,y)$  which can compensate the pressure difference,  $\Delta Cp(x,y)$ .

### 3 Inverse Problem Solver

#### 3.1 Perturbation ( $\Delta$ -form)

In the present research with the residual-correction concept, the small disturbance equation is assumed to be the approximation of the perturbation of the Navier-Stokes equations. If the variation of the viscous effect and the rotation of the flowfield caused by the  $\Delta f_k(x,y)$  is small enough, that approximation is quite appropriate. The final form of the perturbation equation is integral equations. The original work to combine the residual-correction concept and the integral equation of perturbation was in Ref.(5) and its application to the Navier-Stokes flow was in Ref.(6). Those works were for a single component. Here, the newly formulated integral equation of perturbation<sup>(7)</sup> is used. It has the advantage of taking mutual interaction effect on multi component flowfield.

#### 3.2 Formulation

The objective of the formulation is to build a mathematical model which relates a geometrical correction,  $\Delta f(x,y)$ , to the pressure difference,  $\Delta Cp(x,y)$ . The formulation starts with the transonic small disturbance equation and finally, an integral equation system is to be derived. The final equations are valid for both of incompressible and compressible flows as long as  $M_\infty$  is less than 1.0. One can distinguish the compressibility using  $\beta$  value.

In the case that plural wings ( $kmax$  wings) exists in a flowfield, we have a flow equation for the perturbation velocity potential, augmented by  $kmax$  boundary geometry equations and  $kmax$  boundary surface pressure equations. First, the coordinate system is transformed according to the Plandtl-Glauert transformation. Then, the flowfield is described by the small disturbance equation;

$$(\Delta\phi)_{xx} + (\Delta\phi)_{yy} + (\Delta\phi)_{zz} = \frac{\partial}{\partial x} \left( \frac{1}{2} [(\phi)_x + (\Delta\phi)_x]^2 - \frac{1}{2} (\phi)_x^2 \right) \quad (1)$$

The pressure coefficients on each wing surfaces are expressed as

$$\Delta Cp_{k\pm}(x, \frac{y}{\beta}) = -2 \frac{\beta^2}{K} \Delta\phi_x(x, y, c_k \pm 0) \quad (2)$$

$(k = 1, 2, \dots, k \max)$

The flow tangency condition on each wing can be written as

$$(\Delta\phi(x, y, c_k \pm 0))_z = \frac{\partial}{\partial x} (\Delta f_{k\pm}(x, y)) \quad (3)$$

$(k = 1, 2, \dots, k \max)$

The coordinate system for the formulation is that the  $x$ -axis is streamwise, the  $y$ -axis spanwise and the  $z$ -axis is in the thickness direction of the wings. The free stream velocity vector is normalized to be (1, 0, 0). The formulation is performed by applying Green's theorem and calculus. Then, we obtain the theory expressed in a integral equation form shown in the next subsection.

#### 3.3 Final Integral Equations

The theory for the inverse design for multi components in subsonic flows is described as the following integral equation<sup>(8)</sup>. For transonic flows, equations have an extra term which is the volume integral of the transonic nonlinear term (this corresponds to the right hand side of Eq. (1)). Here, because the free stream speed is less than Mach 0.3 for the high-lift devices, the nonlinear term can be neglected. The theory relates the geometry  $\Delta ws$  and  $\Delta wa$  to the function of pressure,  $\Delta us$  and  $\Delta ua$ . A similar system for a supersonic single wing has been developed and applied to practical design<sup>(9)</sup> by one of the authors. The physical meanings of  $\Delta ws$  and  $\Delta wa$  are  $x$  derivative of thickness change and that of camber curve change, respectively. Then, The correction of each surface geometry is expressed as

$$\frac{\partial}{\partial x} \Delta f_{\pm}(x, y) = 1/2(\Delta wa \pm \Delta ws).$$

The  $z$  coordinate of the leading edge of the component  $k$  is  $c_k$ .

$$\begin{aligned} \Delta us_k(x, y) = & -\frac{1}{2\pi} \iint_{S_{kw}} \psi_x(x, y, c_k; \xi, \eta, c_k) \cdot \Delta ws_k(\xi, \eta) d\xi d\eta \\ & -\frac{1}{2\pi} \sum_{p \neq k} \iint_{S_{kw}} \left\{ \begin{array}{l} \psi_x(x, y, c_k; \xi, \eta, c_p) \cdot \Delta ws_p(\xi, \eta) - \\ \psi_s(x, y, c_k; \xi, \eta, c_p) \cdot \Delta ua_p(\xi, \eta) \end{array} \right\} d\xi d\eta \end{aligned} \quad (4)$$

$$\begin{aligned} \Delta wa_k(x, y) = & \frac{1}{2\pi} \iint_{S_{kw}} \left\{ \frac{\Delta ua_k(\xi, \eta)}{(y-\eta)^2} \cdot \left( 1 + \frac{x-\xi}{\sqrt{(x-\xi)^2 + (y-\eta)^2}} \right) \right\} d\xi d\eta \\ & + \frac{1}{2\pi} \sum_{p \neq k} \iint_{S_{kw}} \left\{ \begin{array}{l} \frac{\Delta ua_k(\xi, \eta)}{(y-\eta)^2 + \bar{c}_{k,p}^2} \cdot \\ \left( 1 + \frac{x-\xi}{\sqrt{(x-\xi)^2 + (y-\eta)^2 + \bar{c}_{k,p}^2}} \right) \end{array} \right\} d\xi d\eta \\ & -\frac{1}{2\pi} \sum_{p \neq k} \iint_{S_{kw}} \psi_z(x, y, c_k; \xi, \eta, c_p) \cdot \Delta ws_p(\xi, \eta) d\xi d\eta \end{aligned}$$

$$-\frac{1}{2\pi} \sum_{p \neq k} \iint_{S_{kw}} \Delta ua_p(\xi, \eta) \bar{c}_{k,p}^2 \left( (y-\eta)^2 + \bar{c}_{k,p}^2 \right)^{-2} \cdot (2+3q-q^3) d\xi d\eta \quad (5)$$

where

$$\Delta us_k = -\frac{K}{2\beta^2} [\Delta Cp_+(x, \frac{y}{\beta}, c_k) + \Delta Cp_-(x, \frac{y}{\beta}, c_k)]$$

$$\Delta ua_k = -\frac{K}{2\beta^2} [\Delta Cp_+(x, \frac{y}{\beta}, c_k) - \Delta Cp_-(x, \frac{y}{\beta}, c_k)]$$

$$\psi(x, y, z; \xi, \eta, \zeta) = \frac{1}{r} = \frac{1}{\sqrt{(x-\xi)^2 + (y-\eta)^2 + (z-\zeta)^2}}$$

$$q = \frac{x-\xi}{\sqrt{(x-\xi)^2 + (y-\eta)^2 + \bar{c}_{k,p}^2}}$$

$$\text{and } \bar{c}_{k,p} = c_k - c_p.$$

The second term of Eq.(4), the second, third and forth terms of Eq.(5) express the mutual interaction between the component  $k$  and the others. In these terms,  $\Sigma$  means to take the sum of all  $p$  except  $p$  equal to  $k$ . The area of integration is on the component  $k$  surface.

### 3.4 Discretization for Numerical Computation

To simplify the integral operation over the surface  $S_{kw}$  and  $S_{pw}$  in Eqs.(4) and (5), those are reduced to the integrals on the mean plane of each wing/component. Then, the mean planes are discretized into panels of small interval of  $x$  and  $y$  (Fig. 3). The integral equations yield to linear algebraic ones that are numerically solved. It is easy to impose geometric constraints on the linear equations.

## 4 Present Design System

To design multi element high lift devices, the analysis part of the design system should handle complex geometry. In this research, the CFD simulation process using unstructured mesh<sup>(10)</sup> has been incorporated into the system as shown in Fig. 4 so that the design can be conducted efficiently. Another characteristic of the system is that the gap can be controlled by empirical knowledge.

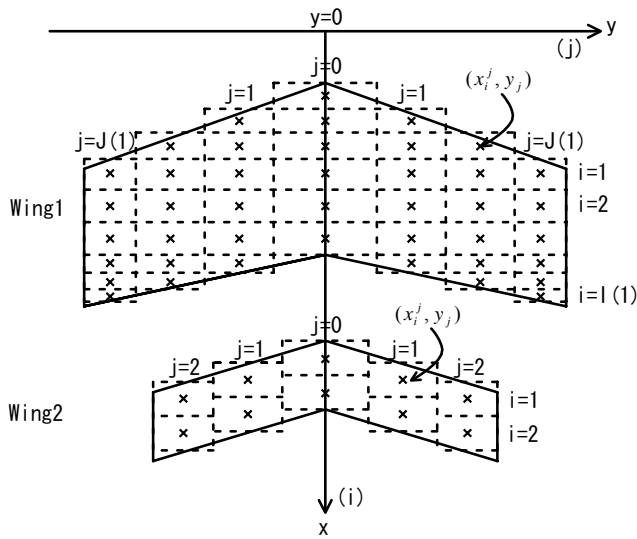


Fig.3 Discretization of wing surface.

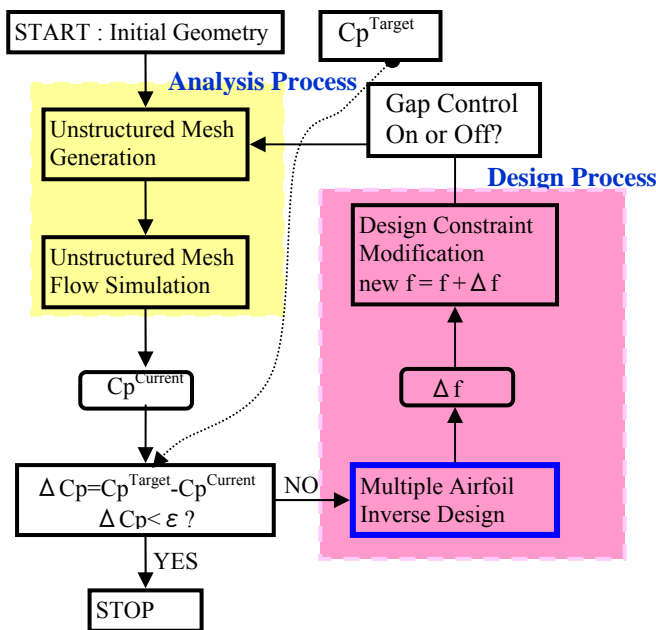


Fig. 4 Design system with unstructured CFD.

#### 4.1 Unstructured Mesh Generation

In this research, mesh generation is done using geometry-adaptive refinement strategy<sup>(11)</sup>. At first, a computational domain is divided into rather coarse Cartesian meshes. Then, quadrilateral cells that include the airfoil surface boundary are divided into four quadrilateral cells. This refinement procedure is repeated until the minimum cell size becomes less than a

specified threshold value. For the viscous region, high aspect ratio (very thin) cells, those which are commonly used with structured mesh generation, are located. Therefore, one can have refined mesh in the normal direction to the surface. For computations, each quadrilateral cell is regarded as two triangular cells. Figure 5 shows the generated mesh around a three element airfoil. For the present design, the minimum spacing is  $3 \times 10^{-5}$ . The total number of triangular elements is 83,730 and that of mesh points is 42,534. For this mesh generation, it takes about five minutes with 3.0GHz Pentium4 processor PC.

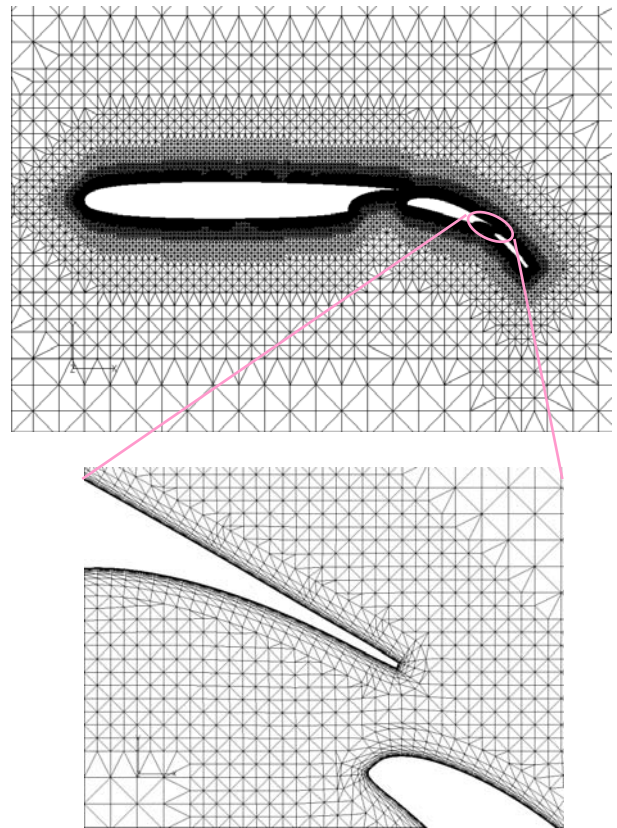


Fig. 5 Unstructured mesh for Navier-Stokes computation.

#### 4.2 Flow Solver Algorithm

The Navier-Stokes equations are solved by a finite volume cell-vertex scheme for arbitrary shaped cells<sup>(12)</sup>. The control volume is of dual cells with no overlap constructed around each

node. The Euler equations for compressible flows are written in an integral form as follows,

$$\frac{\partial}{\partial t} \int_{\Omega} \mathbf{Q} dV + \int_{\partial\Omega} \left( \mathbf{F}(\mathbf{Q}) - \frac{M_{\infty} \sqrt{\gamma}}{\text{Re}} \mathbf{G}(\mathbf{Q}) \right) \cdot \mathbf{n} dS = 0 \quad (1)$$

where  $\mathbf{Q} = [\rho, \rho u, \rho v, \rho w, e]^T$  is the vector of conservative flow variables,  $\rho$  the density,  $u, v, w$  the velocity components in the  $x, y, z$  directions and  $e$  the total energy. The vector  $\mathbf{F}(\mathbf{Q})$  represents the inviscid flux vector and  $\mathbf{n}$  is the outward normal of  $\partial\Omega$  which is the boundary of the control volume  $\Omega$ . For flow simulation, the equations are solved by a finite-volume cell-vertex scheme, and Eq. (1) can be written in an algebraic form as follows,

$$\frac{\partial \mathbf{Q}_i}{\partial t} = -\frac{1}{V_i} \left[ \sum_{j(i)} \Delta S_{ij} \mathbf{h}(\mathbf{Q}_{ij}^+, \mathbf{Q}_{ij}^-, \mathbf{n}_{ij}) - \sum_{j(i)} \Delta S_{ij} \mathbf{G}(\mathbf{Q}_{ij}, \mathbf{n}_{ij}) \right] \quad (2)$$

where  $\Delta S_{ij}$  is the segment area of the control volume boundary associated with the edge connecting points  $i$  and  $j$ . The term  $\mathbf{h}$  is an inviscid numerical flux vector normal to the control volume boundary, and  $\mathbf{Q}_{ij}^+, \mathbf{Q}_{ij}^-$  are values on both sides of the control volume boundary. The subscript of summation,  $j(i)$  means all node points connected to node  $i$ . The numerical flux  $\mathbf{h}$  is computed using an approximate Riemann solver of Harten-Lax-van Leer-Einfeldt-Wada (HLLW). The second order spatial accuracy is realized by a linear reconstruction of the primitive gas dynamic variables with Venkatakrishnan's limiter. The lower/upper symmetric Gauss-Seidel implicit method for the unstructured grid is used for the time integration.

The calculations in the analysis part are of all turbulent. As a turbulence model, The Goldberg Ramakrishnan model<sup>(13)</sup> is used because it does not need to measure a distance from wall.

## 5 Design Example

### 5.1 Multi-element Airfoil for High-lift

The method will be applied to the design of airfoils consisting of three components shown in Fig. 5. In this article, two of three components were designed to realize high lift. As a demonstration, we simplified the problem. We considered two airfoils interacting with each other. The flow condition was that the free stream Mach number is 0.2 and the Reynolds number is 6 million. Initially, two airfoils were of the NACA0012 shape with 0 degree of the angle of attack and had surface pressure distribution indicated by blue solid lines as seen in the upper left graph in Fig. 6, where the given target pressure is plotted with red circles. The chord length of the first airfoil was 1.0 while that of the second one was 0.35. The overlap width and Gap were 0.1 and 0.05, respectively.

### 5.2 Design Process

Figure 6 presents the design process history. The specified target pressures drawn with red circles were prescribed according to the suggestion of Ref.(14). In Fig. 6, the first graph titled by 'iteration 00' shows the initial pressure distribution and geometry contour of each airfoil. From left to right and upper to lower are presented current pressure distributions of blue lines and geometry contours at each iteration step of the design loop. At the initial stage, the lift of the main part is slightly positive, and that of the flap is definitely negative. This fact implies that there is aero-dynamic interaction between the two airfoils.

By performing only five iterations of the design loop, the design was completed. In the lower right graph of Fig.6, the designed geometry and its pressure distribution of blue lines, which excellently agree with the target of red circles, are plotted. For the present design, totally, 200 control points are used to precisely present the two airfoils shape. This means at each iteration step of the design loop, 200 integral equations were solved in the design part (Inverse problem solver) considering  $200 \times 200$

# AN EFFICIENT INVERSE AERODYNAMIC DESIGN METHOD FOR MULTI COMPONENT DEVICES

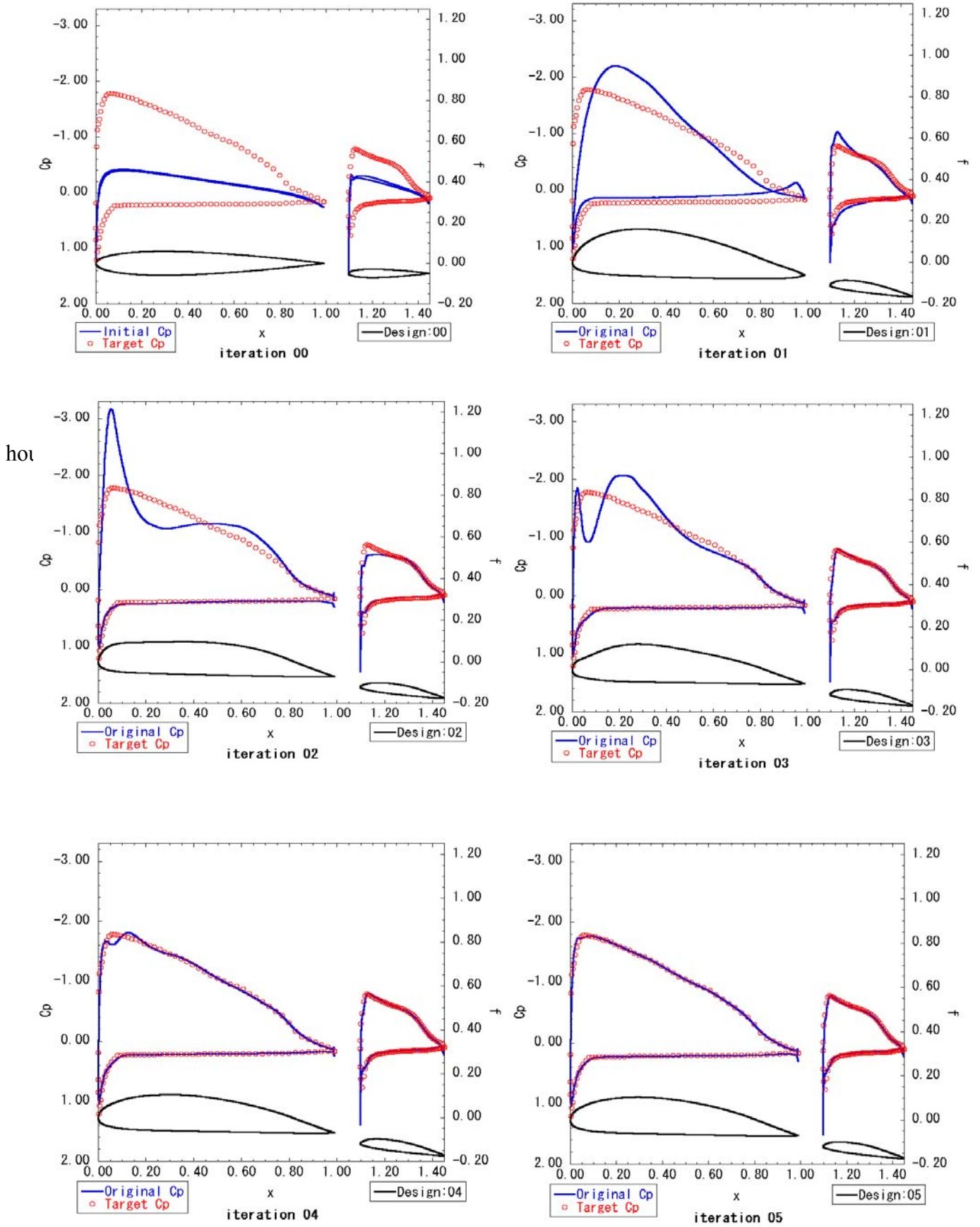


Fig. 6 Design history from initial state to 5<sup>th</sup> iteration step.

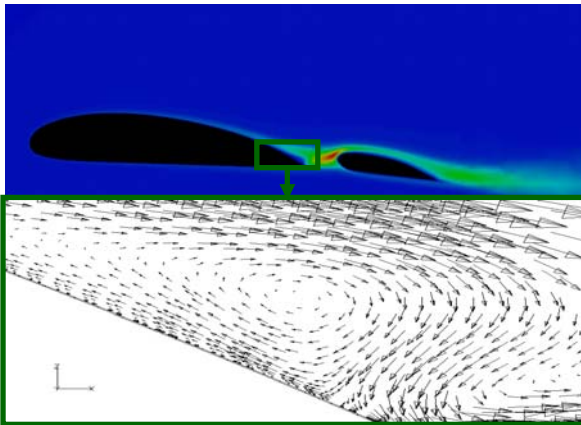


Fig. 7 Vorticity distribution and velocity vectors near trailing edge without gap consideration.

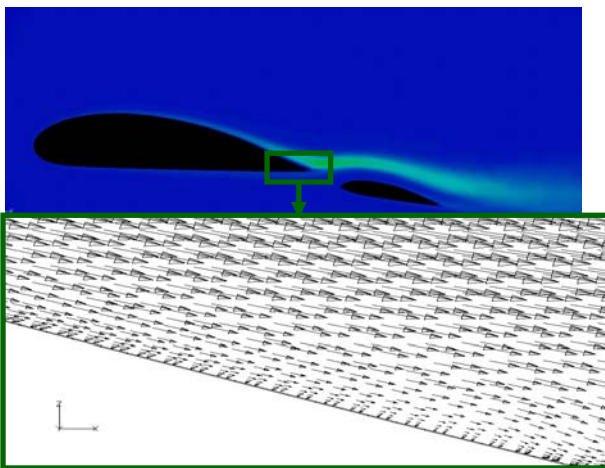


Fig. 8 Vorticity distribution and velocity vectors near trailing edge with gap consideration.

interactions. Observing the history of pressure distribution, the convergence process of the main part is rather unstable compared with the design experience of single airfoil examples. Interestingly, the flap geometry has reached the converged state much earlier than the main part. Finally, the first airfoil has come to take 4.6 degree angle of attack, and the flap has come to take 9.8 degree angle of attack. Both shapes have greatly changed from the initial ones. The designed shapes look good candidate for a conventional high-lift device. It has been shown that the method works well on the design of two-element high-lift devices.

The design system can also control the gap width between components. In the present

system, we found its appropriate value between the trailing edge of the first airfoil and the leading edge of the second one after the first iteration of the design loop. The appropriate value was obtained by parametric studies with the currently realized configuration. After second iteration, we fixed the gap width at the value. The value maximized total lift. The gap width also resulted in low momentum loss of the flow around airfoils, which yielded to low drag. It is confirmed in Figs.7 and 8. Fig. 7 shows the design result without controlling the gap. The second airfoil is in the wake of the first one. It causes separation in the vicinity of the trailing edge of the first airfoil and high pressure region near the Leading edge of the second one. Figure 8 is the design result with adjusting the gap. The vortical wake is avoiding the second airfoil, so the fresh flow can go through the gap between two airfoils. This leads to high lift and low drag.

One iteration in the design loop took about 6 hours. Therefore, this design was completed within two days on 3.0GHz Pentium4 single processor PC. Required memory is less than 512 Mbytes.

## 6 Conclusions

An inverse design method for multi-component aerodynamic devices was systemized on an ordinary PC. The PC inverse design system was applied to preliminary design problems to show the feasibility and efficiency. It has been confirmed that the method works well for the design of airfoil shapes of multiple wing systems. Through the article, the following facts have been seen:

- 1) The present formulation can account for the effect of the thickness, the camber, the angle of attack and the altitude location of each wing.
- 2) The inverse design method is able to evaluate interacting effects among wings accurately and provide design results relevant to the effect.
- 3) The method is so efficient in computational time and memory that it is promising for design problems even the design would be more complicated.

- 4) The method is effective for a wide range of flowfields such as transonic, subsonic and low-subsonic.
- 5) The method can design largely deformed shapes from the baseline.

## References

- [1] C. P. van Dam. The aerodynamic design of multi-element high lift systems for transport airplanes, *Progress in Aerospace Sciences*, Vol. 38, No. 2, pp. 101-144, 2002.
- [2] <http://www.flug-revue.rotor.com/FRHeft/FRH010/FR010e.htm>.
- [3] J.B. Vos, A. Rizzi, D. Darracq, E.H. Hirschel. Navier-Stokes solvers in European aircraft design, *Progress in Aerospace Sciences*, Vol. 38, pp. 601-697, 2002.
- [4] A. Fredeani, M. Chiarelli, A. Longhi, E. Troiani. The lifting system with minimum induced drag, *Notes on Numerical Fluid Mechanics "Aerodynamic Drag Reduction Technologies"*, Vol. 76, Springer, pp. 312-319, 2001.
- [5] S. Takanashi. Iterative three dimensional transonic wing design using integral equations, *Journal of Aircraft*, Vol. 22, No. 3, pp. 655-660, 1985.
- [6] N. Hirose, S. Takanashi, N. Kawai. Transonic airfoil design based on Navier-Stokes equation to attain arbitrary specified pressure distribution, AIAA paper 85-1592, 1985..
- [7] K. Matsushima, S. Takanashi, T. Iwamiya. Inverse design method for Transonic multiple wing systems using integral equations. *Journal of Aircraft*, Vol. 34, No. 3, pp. 322-329, 1997.
- [8] K. Matsushima, T. Iwamiya. An aerodynamic design method for multiple-element wing using inverse problems. *Inverse Problem in Engineering Mechanics*, 1<sup>st</sup> edition, Elsevier, pp. 417-425, 1998.
- [9] K. Matsushima, T Iwamiya, K. Nakahashi. Wing design for supersonic transports using integral equation method, *Engineering Analysis with Boundary Elements*, Vol. 28, pp. 247-255, 2004.
- [10] L. S. Kim, K. Nakahashi. Navier-Stokes Computations of Multi-Element Airfoils, *CFD Journal*, Vol. 12 No. 1, pp. 107-114, 2003.
- [11] K. Nakahashi, K. Egami. An automatic Euler solver using the unstructured upwind method, *Computers & Fluids*, Vol. 19, No. 3/4, pp. 273-286.
- [12] D. Sharov, K. Nakahashi. Reordering of hybrid unstructured grid for lower-upper symmetric Gauss-Seidel computations, *AIAA Journal*, Vol. 36, No. 3, pp.484-486, 1998.
- [13] U. C. Goldberg, S. V. Ramakrishnan. A Pointwise Version of Baldwin-Barth Turbulence Model, *Comp. Fluid Dyn.* Vol. 1, pp.321-338, 1993.
- [14] M. Shigemi. A solution of inverse problems for multi-element aerofoils through application of panel method, *Trans. Japan Society for Aerospace Sciences*, Vol. 28, No. 80, pp., 1985.